Desalination and Water Treatment
www.deswater.com

doi: 10.5004/dwt.2023.29858

306 (2023) 208–219
September

Remediation of metribuzin (herbicide) from aqueous solution using turnip peel biomass-based zinc oxide nanocomposite

Muhammad Zahoor[a,*], Azmat Ullah[b], Zakir Ullah[b], Muhammad Abbas[b], Ali Shan[b], Riaz Ullah[c], Muhammad Naveed Umar[d], Sher Wali Khan[e]

[a]*Department of Biochemistry, University of Malakand, Chakdara Dir Lower, 18800. Khyber Pakhtunkhwa, Pakistan, email: mohammadzahoorus@yahoo.com*
[b]*Department of Chemistry, Govt Degree College Mingora, Swat, Khyber Pakhtunkhwa, Pakistan, emails: azmatullah9499@gmail.com (A. Ullah), zakirkhan55505@gmail.com (Z. Ullah), muhammadabbasba244@gmail.com (M. Abbas), alishan03409391325@gmail.com (A. Shan)*
[c]*Department of Pharmacognosy, College of Pharmacy, King Saud University, Riyadh 11451, Saudi Arabia, email: rullah@ksu.edu.sa*
[d]*Department of Chemistry, University of Liverpool, UK, email: m.naveed-umar@liverpool.ac.uk*
[e]*Department of Chemistry, Shaheed Benazir Bhutto University, Dir Upper Khyber Pakhtunkhwa, Pakistan, email: sherwalikhn@yahoo.co.uk*

Received 16 May 2023; Accepted 17 August 2023

ABSTRACT

A novel biosorbent/nanocomposite was prepared from the turnip peel precursors and zinc oxide. The turnip peels biomass zinc oxide nanocomposite (TPZnOnc) was used for the remediation of metribuzin (MEB) pesticide from aqueous solution. The prepared nanocomposite was characterized using scanning electron microscopy, X-ray diffraction and Fourier-transform infrared spectroscopy techniques. The point of zero charge (pH_{pzc}) of TPZnOnc was determined using mass titration method. Batch sorption approach was utilized to study the sorption capability of MEB molecules from aqueous media. The removal of MEB from solution by TPZnOnc was studied as a function of time, initial concentration of MEB, pH and adsorbent dosage. The optimum pH for the removal of MEB was found to be 3 whereas the optimum dosage of TPZnOnc to be utilized was 600 mg/30 mL. The surface saturation of TPZnOnc with MEB molecules occurred in 1 h (equilibration time). The maximum sorption of MEB molecules occurs at initial concentration of 80 mg·L^{-1}. Out of the utilized kinetics models, pseudo-second-order kinetic model fitted the data well with high regression constant value. Various isotherm models were applied to the sorption isotherm data. Langmuir adsorption isotherm model was found to be the best one to fit the data well with high regression constant value whereas the maximum sorption capacity (X_{max}) calculated was 19.20 mg·g^{-1}. Various thermodynamic parameters were calculated from Van't Hoff plot. Negative values of $\Delta G°$ shows that the process of sorption is spontaneous. The value of $\Delta G°$ lies in the range of –75 to –400 kJ·mol^{-1} suggest that the removal of MEB molecules on the surface of TPZnOnc is chemical process. Negative value of $\Delta H°$ (–82.56 kJ·mol^{-1}) confirmed that the removal process of MEB molecules onto the surface of TPZnOnc is exothermic whereas the negative value of $\Delta S°$ confirmed that the randomness decreases at the solid–liquid interface during sorption MEB molecules on the surface of TPZnOnc.

Keywords: Adsorption; Nanocomposite; Herbicides; Turnip peel precursors; Zinc oxide

* Corresponding author.

1. Introduction

Fruits and vegetables are the commodities in human diet that are consumed on large scale. They contain significant amounts of dietary fiber, minerals, and vitamins etc. With the increasing human population there is need to get more production per land unit. Fertilizers and pesticides are utilized worldwide to increase crops production and exclusion of pests, to shield fruits and vegetables from variety of diseases [1,2]. Nevertheless, pesticides have a large number of benefits for fruits and vegetables but still they are considered as fatal chemicals. As the pesticides are largely used inadequately and haphazardly, therefore they are considered as environmental hazards. The uncontrolled usage of pesticides may end up in extensive discharge to the environment. They not only disturb the human health but likewise disturb the biomes as well [3].

Triazinone is a class of herbicide used worldwide for herbs control. Metribuzin (MEB) belong to this class of herbicide. Its chemical name is 4-amino-6-tertiary-butyl-4,5-dihydro-3-methylthio-1,2,4-triazin-5-one (Fig. 1). MEB is commonly utilized as the pre- and post-emergent treatment of unwanted grasses. They are also used for the control of broadleaved wildflowers in diverse crops such as tomatoes, soya beans, sugarcane, barley, potatoes, maize and alfalfa [4]. MEB is highly soluble in water, its solubility is 1,000–1,100 mg·L^{-1}. Its absorption capability in soil texture is very low which makes it more hazardous to aquatic environment as reported [5–8].

The entry sources of MEB to aquatic environment are: spraying, leaking and flowing from treated agricultural land, and unintended expulsion etc. All these sources leads to contamination of aquatic environment. The presence of MEB in aquatic environment have an adverse impact on algae and freshwater aquatic plants. It also disrupts the normal functioning of aquatic fauna as it disrupts their endocrine systems [9]. As a result, the Environmental Protection Agency of USA has recommenced a precise concentration as 170–180 μg·L^{-1} of MEB in drinking water [10–12].

Currently, several processes have been employed for the remediation of pesticides from aquatic media. These methods are photo-Fenton method [13], membrane separation [14], photo degradation in the presence of catalyst [15], advanced oxidation processes, ozonation and anaerobic degradation [15–17]. All these methods have a number of drawbacks due to which, they are not been comprehensively used for the remediation of pesticides from aquatic media. Consequently, scientists are giving more consideration to scrutinize new procedures which are cost-effective, and environment friendly. In this scenario, biosorption is one of the most encouraging and substituting procedure. At the same time its cost-effective nature, efficacy and production of little secondary pollutants makes the process more versatile [18]. In biosorption process waste biomass of fruits and vegetables are usually employed as they contain a number of functional groups to which the contaminant binds from aquatic media which are then disposed of [19]. Formerly, a large number of biosorbents have been employed for the remediation of pesticides from aqueous solutions such as neem peels powder [20], pumpkin seeds peel powder [21], pea peels [22], cork species [23], coal fly ash [24], bark [25], straw [26] and activated carbon [27].

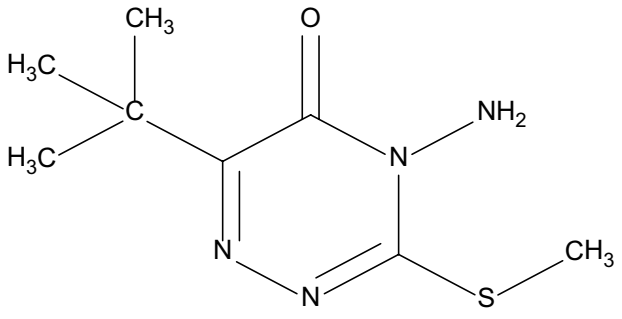

Fig. 1. Structure of metribuzin.

Most of the biosorbents have soft nature. They have the ability to form gel like structure in aquatic media. They have numerous sorption active spots on their surfaces [28]. It has been recognized to enhance the sorption capacity of sorbents by various methods. Therefore, attempts have been made to intensify the sorption capacity of sorbents. But sorbents obtained from biomass impregnated with metal oxides have more advantages than unimpregnated biomass precursors. As biomass impregnated with metal oxide have comparable surface area and tiny particle size. Moreover, they give toughness and durability to polymeric ingredients of biomass precursors [29–32].

Keeping in view the aforementioned of biomass-based adsorbents, herein an attempt was made to synthesize turnip (*Brassica rapa*) peels-zinc oxide nanocomposite (TPZnOnc) for the remediation of MEB from aqueous solutions. The biosorption of MEB from aqueous solution was examined as a function of contact time, initial MEB concentration, TPZnOnc dosage, and pH to attain optimum experimental conditions for the uptake of MEB molecules from aqueous solutions.

2. Material and methods

2.1. Biosorbent

Purple-top white globe turnips of Kalam valley were collected from the local market in Swat, Pakistan which are considered to be a rich source of isothiocyanates and glucosinolates. Beside these components' indoles, phenolic and flavonoids etc. are also present. The peel of this commodity was used as raw biosorbent material.

2.2. Herbicide

Analytical grade metribuzin (herbicide) of 99% purity was purchased from the Syngenta (Pakistan). The characteristic features of the metribuzin are tabulated in Table 1. The other chemicals and reagents used in the experimental work were of analytical grade and were acquired from local market. Double distilled water was used throughout the experimental work.

2.3. Preparation of TPZnOnc

In a conical flask 0.75 g of zinc oxide (ZnO), accurately weighed was dissolved in 10 mL of 65% nitric acid (HNO_3)

Table 1
Kinetics parameters of the sorption of metribuzin onto TPZnOnc

Pseudo-first-order			Pseudo-second-order			Intraparticle diffusion		
$X_{Experimental}$ $X_{Calculated}$	K_1	R^2	$X_{Experimental}$ $X_{Calculated}$	K_2	R^2	K_3	C	R^2
9.60 mg·g^{-1} 1.15 mg·g^{-1}	2.3	0.9562	9.60 mg·g^{-1} 10.60 mg·g^{-1}	0.0393 0.0355	0.9942	1.34	1.51	0.9917

and 100 mL of 1% acetic acid (CH_3COOH) solution mixture. About 10 g of dried turnip peel powder was added to flask containing dissolved ZnO and sonicated for 30 min. After sonication, 1.0 N sodium hydroxide (NaOH) was added dropwise from a burette to the mixture till the pH of slurry reached to 10. The flask containing mixture was then kept in a thermostat at 333 K for 3 h. The pH of the resultant contents was brought to neutral using 1 N HCl and then repeatedly washed with distilled water. Finally, the sample was dried at 323 K in an oven for 1 h. The dried sample was pulverized into fine powder and then stored in a sealed glass bottle. The whole process has been summarized in Fig. 2.

2.4. Characterization of TPZnOnc

The prepared sample was characterized by X-ray diffraction (XRD), scanning electron microscopy (SEM), Fourier-transform infrared (FTIR) spectroscopy and mass titration method for pH_{pzc}.

2.5. Biosorption studies

The kinetics of MEB on the surface of TPZnOnc was studied as a function of time where 0.6 g of TPZnOnc was added to a glass reagent bottle containing 30 mL aqueous solution (20 g·L^{-1}) of MEB. The mixture was stirred for different intervals of time at 298 K.

About 20 mg·L^{-1} of MEB solution was also stirred without TPZnOnc to notice some sorption of herbicides on the bottles inside surface or degradation during the equilibration during shaking. After specified interval of time the slurry was centrifuged at 2,000 rpm for 10 min. The quantity of MEB was calculated in the supernatant. The extent of MEB sorbed by the TPZnOnc was calculated from the difference of initial concentration (Q_i) and final concentration (Q_f) in the supernatant.

In the blank (without bio sorbent) no adsorption of MEB occurs on glass walls of reagent bottles.

During adsorption isotherm studies 30 mL of MEB solutions of different concentration, that is, 30 to 120 mg·L^{-1} were taken in a series of reagent bottles each containing 600 mg of TPZnOnc. The reagent bottles were shaken at 298 K for 1 h. The slurry was centrifuged at 2,000 rpm for 10 min. The quantity of MEB was calculated in the supernatant at 294 nm using a double beam UV/Visible spectrophotometer. The extent of MEB sorbed in each experiment by the TPZnOnc was calculated from the difference of initial concentration (Q_i) and final concentration (Q_f) of in the supernatant.

To check the optimum dose of TPZnOnc for the maximum removal of MEB, the amount of TPZnOnc was varied from 100–1,000 mg in series of bottles containing 30 mg·L^{-1} initial concentration of MEB and stirred for 1 h.

To check the optimum pH for the removal of MEB on the surface of TPZnOnc, the pH of MEB solution was varied from 3 to 10 whereas pH was adjusted with NaOH and HCl solutions.

For the determination of various thermodynamic parameters 600 mg of TPZnOnc (optimum dose) was added to 30 mL MEB solution in 100 mL glass reagent bottles. All the reagent bottles were stirred at 298, 313 and 333 K each for 1 h. After separation of TPZnOnc the MEB concentration in the supernatant was determined using a double beam UV-Visible spectrophotometer at 294 nm.

2.6. Data analysis

The following equations were used to analyze the sorption kinetics, sorption isotherm and mechanism of decontamination of MEB molecules present in aqueous solutions on the surface of TPZnOnc.

$$X_e = \left(Q_i - Q_f\right) \times \frac{V}{m} \tag{1}$$

where Q_i is the initial concentration of MEB in mg·L^{-1}, Q_f is the final concentration of MEB in mg·L^{-1} at time t. X_e is the maximum amount of MEB adsorbed in mg·g^{-1} on the surface of TPZnOnc, V is the volume in liter (L) of MEB solution and W is the amount of TPZnOnc in g.

$$\%\text{Removal} = \frac{\left(Q_i - Q_f\right)}{\left(Q_i\right)} \times 100 \tag{2}$$

Eq. (2) represents the % removal of MEB molecules from aquatic solutions.

2.6.1. Kinetic models

Pseudo-first-order kinetics model:

$$\ln\left(X_e - X_t\right) = \ln X_e - K_1 t \tag{3}$$

Pseudo-second-order kinetics model:

$$\frac{t}{X_t} = \frac{1}{K_2 X_e^2} + \frac{t}{X_e} \tag{4}$$

where X_t and X_e is the amount of MEB biosorbed on the surface of TPZnOnc in mg·g^{-1} at time t and at equilibrium time, respectively. K_1 is the pseudo-first-order

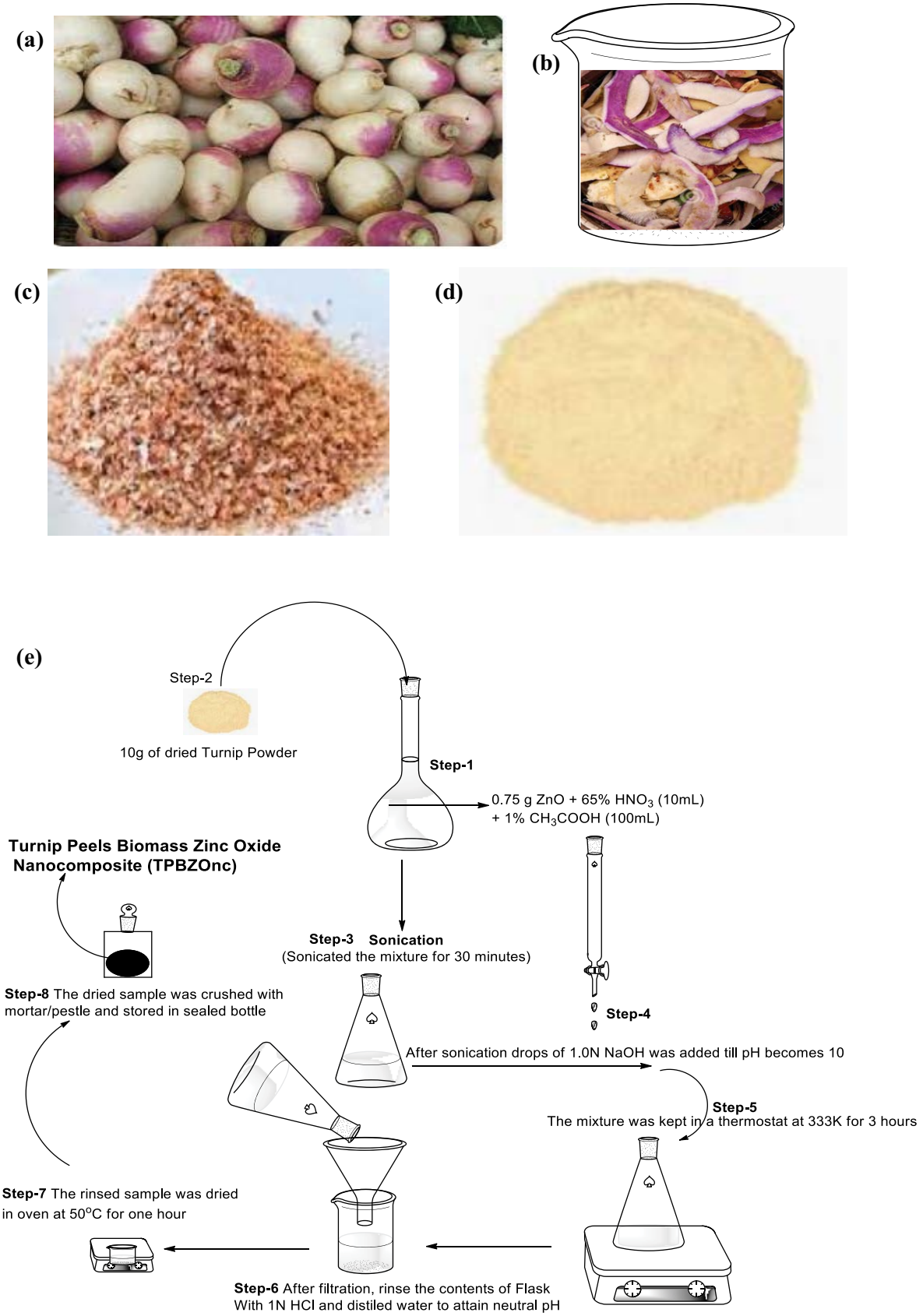

Fig. 2. (a) Purple-top white globe turnips, (b) turnip peels, (c) dried turnip peels in shade, (d) turnip peels powder and (e) schematic diagram of turnip peel biomass zinc oxide nanocomposite (TPZnOnc).

kinetics rate constant in per minute (min^{-1}). In Eq. (4) K_2 is the pseudo-second-order kinetics rate constant in gram per milligram per minute ($g \cdot mg^{-1} \cdot min^{-1}$).

Intraparticle diffusion model:

$$X_t = K_3 t^{0.5} + C \tag{5}$$

where X_t ($mg \cdot g^{-1}$) is the amount of MEB biosorbed at time t, K_3 is the intraparticle diffusion rate constant in $mg \cdot g^{-1} \cdot min^{-1/2}$ and C is the thickness of boundary layer in $mg \cdot g^{-1}$.

2.6.2. Isotherm models

2.6.2.1. Langmuir isotherm model

The linearized form of Langmuir isotherm model is given as:

$$\frac{Q_e}{X_e} = \frac{1}{K_L X_m} + \frac{Q_e}{X_m} \tag{6}$$

where X_e in $mg \cdot g^{-1}$ is the amount of MEB biosorbed at equilibrium time, Q_e in $mg \cdot L^{-1}$ is the equilibrium concentration of MEB. X_m in $mg \cdot g^{-1}$ is the calculated maximum adsorption capacity of TPZnOnc and K_L in $L \cdot g^{-1}$ is the Langmuir constant.

2.6.2.2. Freundlich isotherm model

Freundlich isotherm model gives us information about the heterogeneous system of sorbate–sorbent systems. The logarithmic form of Freundlich isotherm model is given as:

$$\ln X_e = \ln K_F + \ln \frac{Q_e}{n} \tag{7}$$

where X_e in $mg \cdot g^{-1}$ is the amount of MEB biosorbed at equilibrium time, Q_e in $mg \cdot L^{-1}$ is the equilibrium concentration of MEB. K_F and n are the Freundlich constants.

2.6.2.3. Jovanovich isotherm model

Jovanovich isotherm model is constructed on the same statement as of the Langmuir isotherm model, however this isotherm in addition elucidates the mechanical interactions between sorbent and adsorbate molecules [33].

The linear form of Jovanovich isotherm model is given as follows [34]:

$$\ln X_e = \ln X_{\max} + K_J Q_e \tag{8}$$

where X_e is the amount of MEB adsorbed in $mg \cdot g^{-1}$ on the surface of TPZnOnc, Q_e in $mg \cdot L^{-1}$ is the equilibrium concentration of the MEB, X_{max} in $mg \cdot g^{-1}$ is the maximum adsorption capacity of TPZnOnc and K_J is Jovanovich isotherm constant.

2.6.3. Adsorption thermodynamic

The Van't Hoff equation was utilized to conclude various thermodynamic parameters, that is, $\Delta H°$ and $\Delta S°$ of the biosorption process [35]. The linearized form of Van't Hoff equation is given as:

$$\ln K = \frac{\Delta S°}{R} - \frac{\Delta H°}{RT} \tag{9}$$

where $\Delta S°$ is standard entropy, $\Delta H°$ is standard enthalpy, T is the temperature in Kelvin, R is the universal gas constant and K is the distribution constant. The value of K is obtained from the ratio of the amount adsorbed and equilibrium concentration ($K = X_e/Q_e$) [35].

The values of standard free energy ($\Delta G°$) was calculated using the following relation:

$$\Delta G° = \Delta H° - T\Delta S° \tag{10}$$

3. Results and discussions

Fig. 3 shows the SEM photograph of TPZnOnc with the presence of numerous cavities and pores on the surface of biomass as is evident from Fig. 3a. The surface is homogeneous and clear with impregnation of ZnO (Fig. 3b) which have partially filled the cavities and as a result the surface has become heterogeneous and rougher. The particle sizes were in the range from 92 to 95 nm. The Figure shows uniform distribution of ZnO particles on the surface

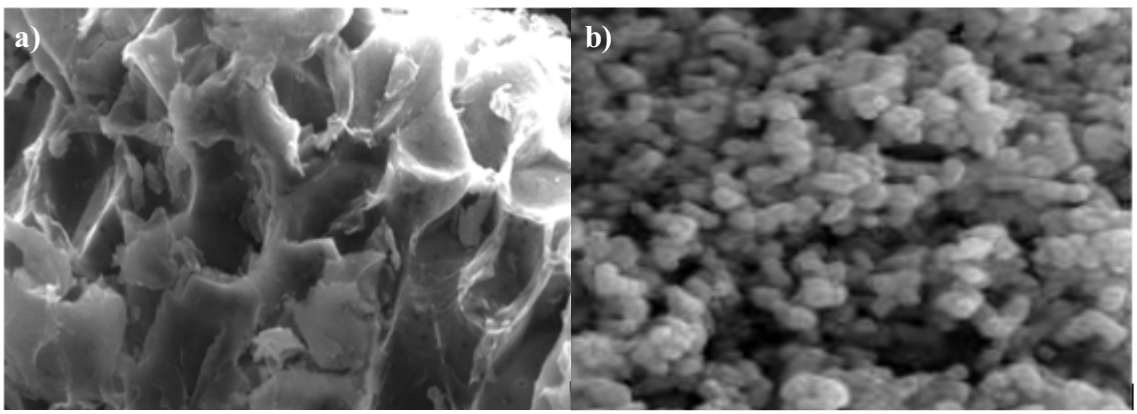

Fig. 3. Scanning electron microscopy image of (a) biomass and (b) TPZnOnc.

of turnip biomass (the cloudy surface). The bright sphere on the surface of TPZnOnc may be due to the presence of moisture.

Fig. 4 shows the XRD diffractogram pattern of TPZnOnc. XRD technique gives us information about the crystallinity or amorphous nature of a sample. The XRD diffractogram of TPZnOnc confirm the crystallinity of nanocomposite. There are sharp and distinctive peaks with narrow width at 2θ°. The values of diffractogram at 2θ° are at 29°, 37.3°, 46°, 48.4° and 67° matches with crystallographic planes of 95, 100, 101, 103 and 200 repectively. All these indices planes confirms the hexagonal crystalline structure of ZnO. The size of the particles determined was 85 nm as calculated from Scherrer equation.

Fig. 5 shows the FTIR spectra of TPZnOnc. There are a number of considerable peaks which represent the presence of large number of functional groups. The broader peak in the range of 3,400–3,370 cm^{-1} corresponds to the interaction of –OH and $–NH_2$ functional group. A peak in the region of 2,200 cm^{-1} corresponds to –CH stretching. There are two peaks in the region of 1,400–1,300 cm^{-1} corresponds to C=C bonds of aromatic rings. The narrow peaks in the region of 1,100–900 cm^{-1} corresponds to –OH alcoholic, –C–O–C– ethereal functional groups, –O–H of water molecules sorbed during formation of nanocomposite and due to hydrogen bonding. The characteristic peak in the region of 450–440 cm^{-1} matches with Zn–O bond of TPZnOnc.

Fig. 6 illuminates the point of zero charge (pH_{pzc}) of TPZnOnc. For the determination of pH_{pzc} a mass titration method was employed. In this method various amount of TPZnOnc was added to fresh distilled water. The TPZnOnc + distilled water mixture was stirred for 24 h in a number of reagent bottles. The resultant pH was noted after 24 h of equilibration. The process was carried out under the atmospheric environment of nitrogen gas. The pH_{pzc} of TPZnOnc was found to be 7.8.

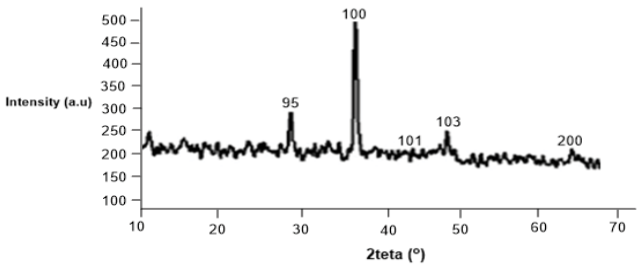

Fig. 4. X-ray diffractogram of TPZnOnc.

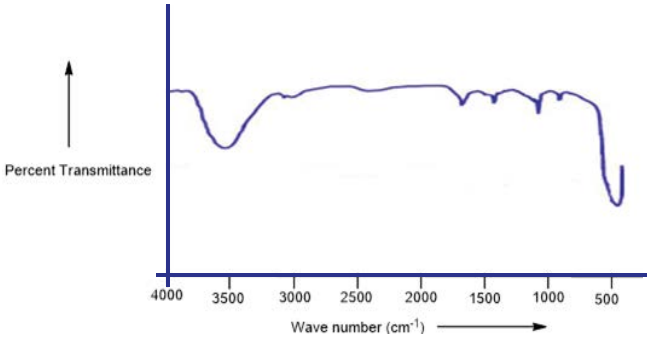

Fig. 5. Fourier-transform infrared spectra of TPZnOnc.

The adsorption kinetics of MEB are shown in Fig. 7a. The rate of adsorption increases gradually with time which is very high in initial 30–35 min where about 70%–75% removal of MEB have occurred. There was no appreciable change in the biosorption of MEB on the surface of TPZnOnc after 1 h. At this time the surface of TPZnOnc is fully saturated with molecules of MEB. Therefore, 1-h time was selected as equilibration time in all proceeding experiments.

Various kinetic models were applied to the sorption kinetics data of MEB. The results showed that pseudo-second-order kinetic model was the best to explain the data. It is clear from Fig. 7c that the line of second-order kinetic model is agreeing well with the experimental data than that of pseudo-first-order kinetic model with the value of regression (R^2) approximately equal to unity. Additionally, the amount of MEB adsorbed theoretically from pseudo-second-order kinetic equation was almost equal to the experimentally determined value (X_e). Whereas, deviation in case of pseudo-first-order kinetics were observed. Various constants were obtained from kinetic models that are tabulated in Table 1.

The intraparticle diffusion model was used to elucidate mechanism of adsorption. The data points in the plot of intraparticle diffusion model shows nearly a linear plot showing the sorption to be a single step process (diffusion-controlled process). The intraparticle diffusion model constants are given in Table 1.

The isothermal studies of MEB onto TPZnOnc were performed as a function of initial concentration of MEB where its concentration was varied from 30 to 120 $mg{\cdot}L^{-1}$. The adsorption isotherm plot of MEB is given in Fig. 8a. The plot shows that the rate of adsorption increases with increase in initial concentration of MEB up to 80 $mg{\cdot}L^{-1}$. After this concentration, no appreciable change was observed in the removal of MEB from aquatic media. At this concentration complete saturation of TPZnOnc surface have occurred and all the active sites on the surface of TPZnOnc are occupied by MEB molecules.

The adsorption isotherm data was then fed to different isotherm models to know the mechanism of sorption. Different plots of isotherm models are given in Fig. 8b–d while, various isotherm parameters obtained from the

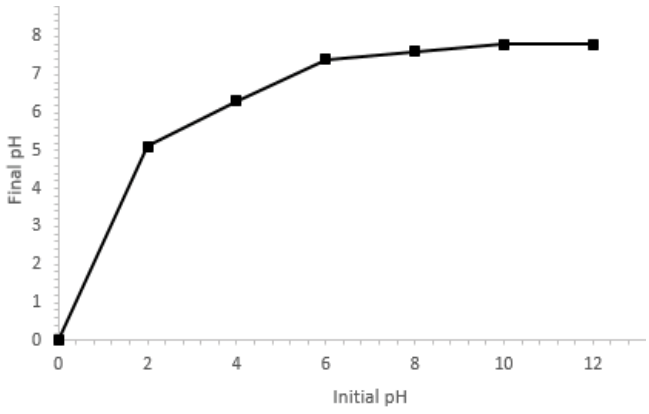

Fig. 6. pH_{pzc} plot of TPZnOnc.

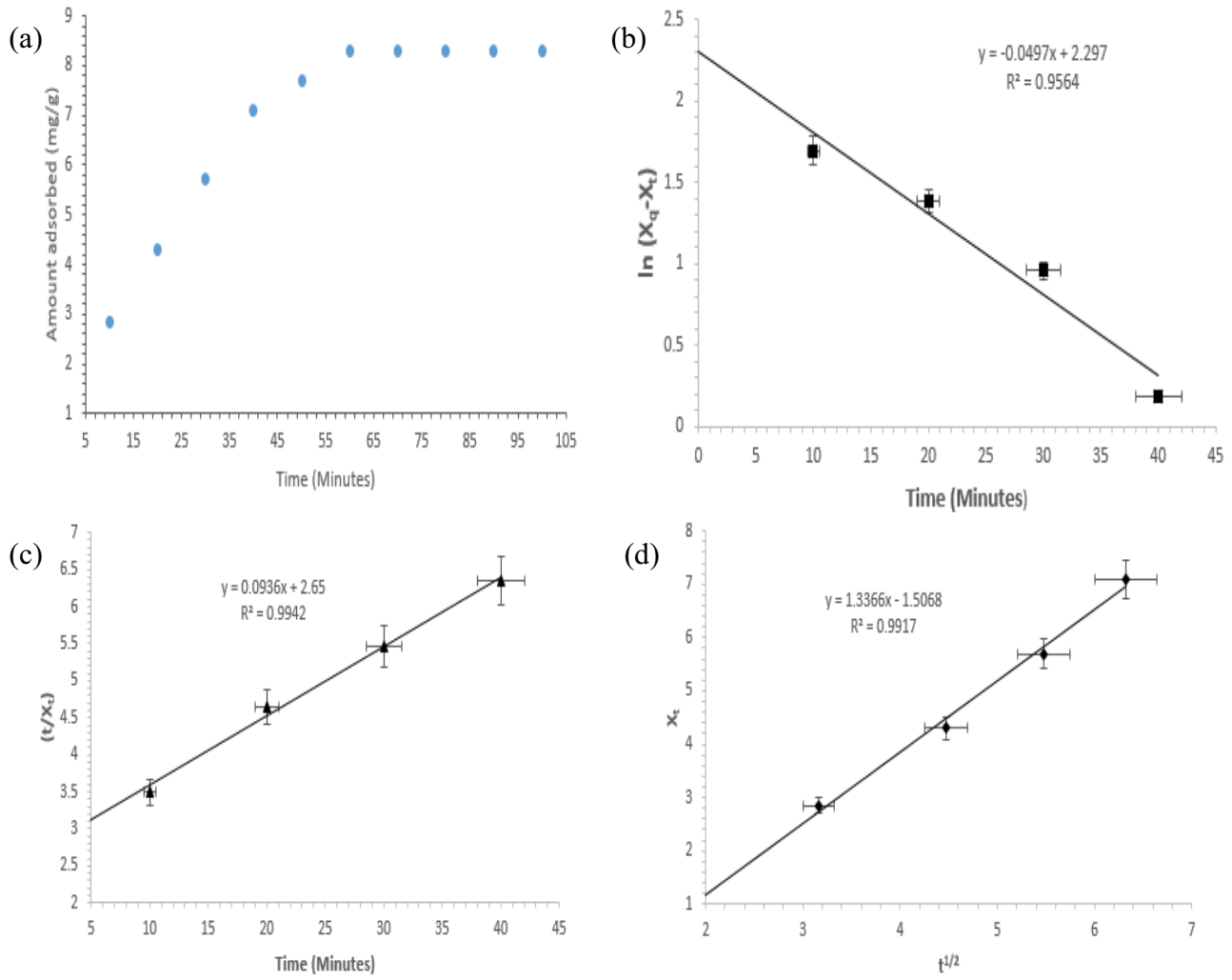

Fig. 7. (a) Adsorption kinetics of metribuzin onto TPZnOnc, (b) pseudo-first-order kinetic model, (c) pseudo-second-order kinetic model and (d) intraparticle diffusion kinetic model.

slopes and intercepts of these plots are tabulated in Table 2.

Langmuir adsorption isotherm model was found best fitted model of isothermal data than Freundlich and Jovanovich model. The maximum sorption capacity (X_{max}) was found approximately equals to the experimentally determined sorption capacity of TPZnOnc. The X_{max} obtained from Langmuir isotherm model was equal to 19.20 mg·g^{-1}. Furthermore, the value of R^2 is almost equal to unity. Also, the value of R_L is greater than zero and less than one (R_L = 0.44) it confirms that the biosorption of MEB onto TPZnOnc is favorable.

Sorbent dose plays an important role in the removal of pollutant molecules from aqueous media during sorption processes. Fig. 9 shows the impact of TPZnOnc dose on the removal of MEB molecule. For this purpose, the initial dosage of TPZnOnc was varied from 100 to 1,000 mg. It is from the plot the percent removal of MEB molecules that there is an increase from 42% (100 mg) to 63% (600 mg) with increase in sorbent dosage. The rise in percent removal of MEB molecule with rise in dose of TPZnOnc is due to the availability of greater number of active sites and larger surface area. It is also clear from the plot that no appreciable change in percent removal of MEB molecule was observed above 600 mg dosage. At this dosage complete saturation of TPZnOnc active sites have occurred. Therefore, 600 mg TPZnOnc was selected as optimum doses for all the subsequent experimental work.

Fig. 10 shows the impact of pH on the remediation of MEB molecules from aqueous solution. pH of media plays an important role in the remediation of contaminants from aquatic media. For this purpose, the initial pH of MEB was varied from 3 to 10. It is clear from the plot that at pH 3 the percent removal of MEB is 59, while at pH 10, the percent removal of MEB molecules has reduced to 22. It shows that as pH increases the percent removal of MEB molecules deceases. Therefore, pH 3 was selected as optimum pH. At low pH the surface of TPZnOnc became cationic and attract the anionic sites of MEB molecules due to electrostatic forces of attraction. As a result, the percent removal of MEB molecules was high (pH < pH_{pzc} surface of TPZnOnc is cationic). The reason for low percent removal of MEB

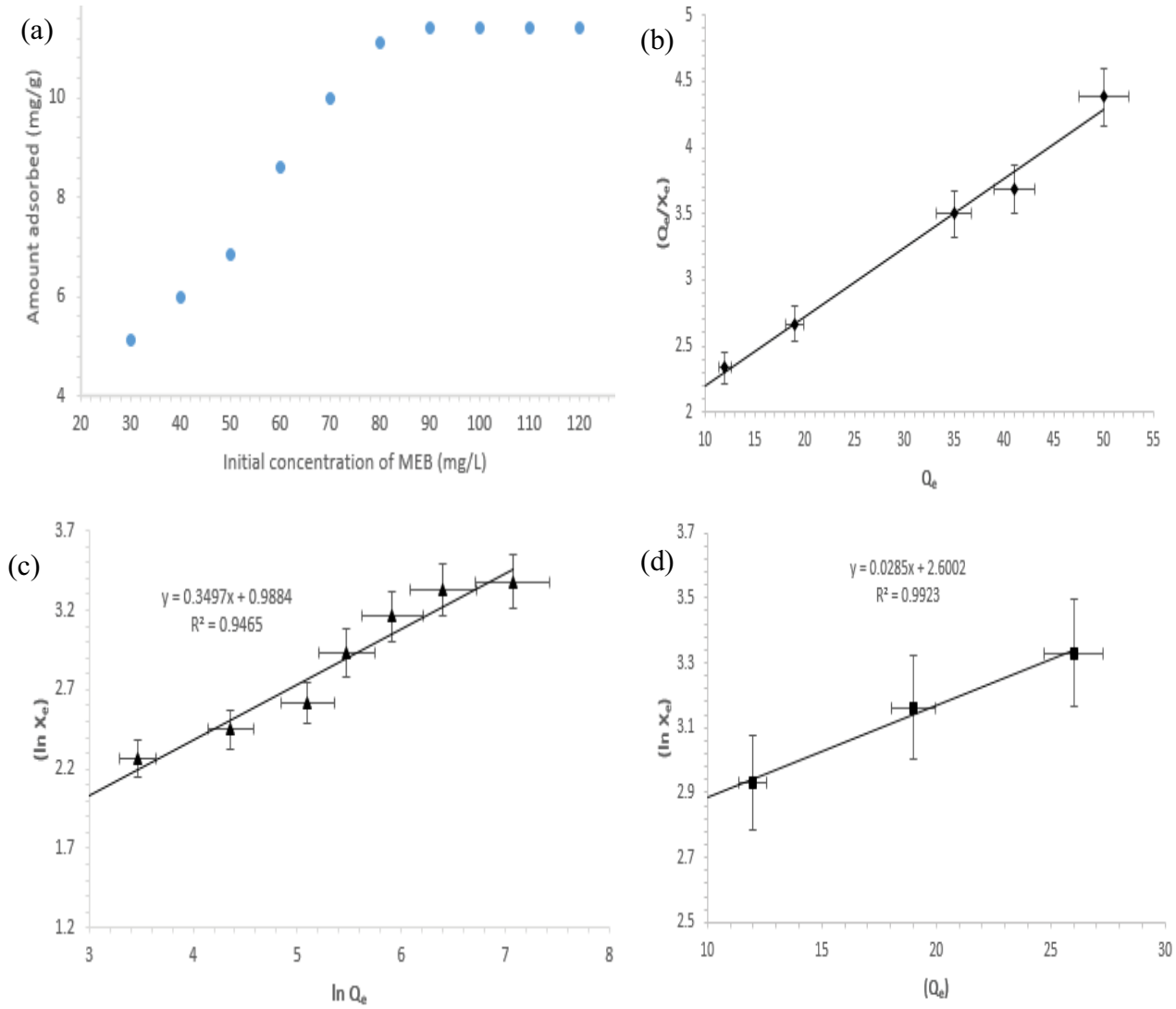

Fig. 8. (a) Adsorption isotherm of metribuzin onto TPZnOnc, (b) Langmuir adsorption isotherm, (c) Freundlich adsorption isotherm and (d) Jovanovich adsorption isotherm.

Table 2
Isotherm parameters of the sorption of metribuzin onto TPZnOnc

Isotherm	Constants	R^2
Freundlich	K_F = 0.01 1/n = 0.35	0.947
Langmuir	K_L = 0.0310 mg·g^{-1} X_{max} = 19.20 mg·g^{-1} R_L = 0.44 dm^3·mol^{-1}	0.99
Jovanovich	K_J = 0.0285 X_{max} = 0.95	0.99

molecules on the surface of TPZnOnc is due to the anionic nature of TPZnOnc. The anionic surface of TPZnOnc repels the anionic sites of MEB molecules (pH > pH_{pzc} surface of TPZnOnc is anionic).

The Van't Hoff graphs (Fig. 11) was obtained by plotting ln$K$ vs. 1/T. Different values of distribution coefficient ($K = X_e/Q_e$) was obtained from the ratio of MEB molecules sorbed on the surface of TPZnOnc and equilibrium concentration of MEB at different temperatures. The values of $\Delta H°$ and $\Delta S°$ were obtained from the slope and intercept of linear plot, respectively using Eqs. (9) and (10).

The values of $\Delta G°$ calculated from equation ($\Delta G° = \Delta H° - \Delta S°$) for the removal of MEB at different temperatures were negative. Negative value of $\Delta G°$ suggest that the process of adsorption is spontaneous (–76.21, –75.78 and –75.36 kJ·mol^{-1} corresponds to 298, 318 and 338 K). These values suggest that lower temperature is a favorable condition for the decontamination of MEB molecules on the surface of TPZnOnc. Similarly, the value of $\Delta G°$ also confirms the type of adsorption to be a chemical one as values falling in the range of 0–20 kJ·mol^{-1} indicate are attributed to physical adsorption processes, while value in the range of 75–400 kJ·mol^{-1} indicates that the process of adsorption

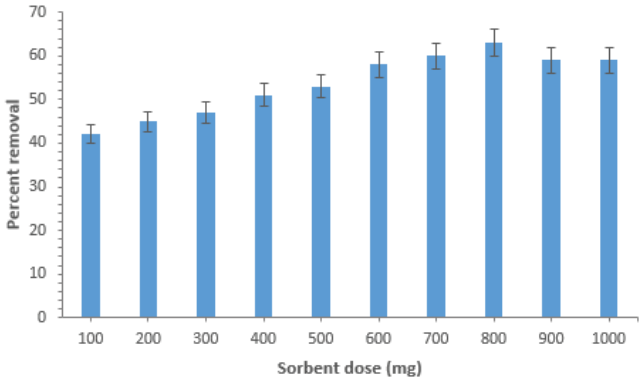

Fig. 9. Effect of TPZnOnc dosage on percent removal of metribuzin.

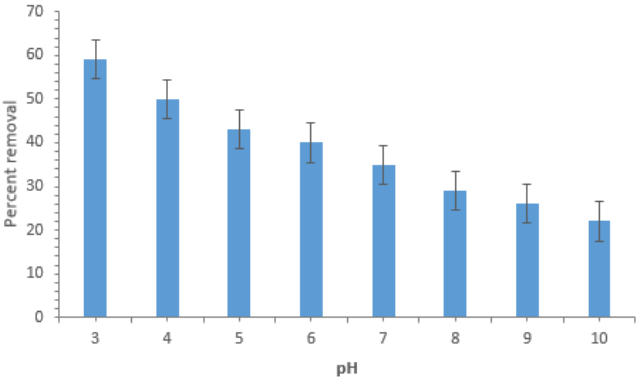

Fig. 10. Effect of initial pH on percent removal of metribuzin.

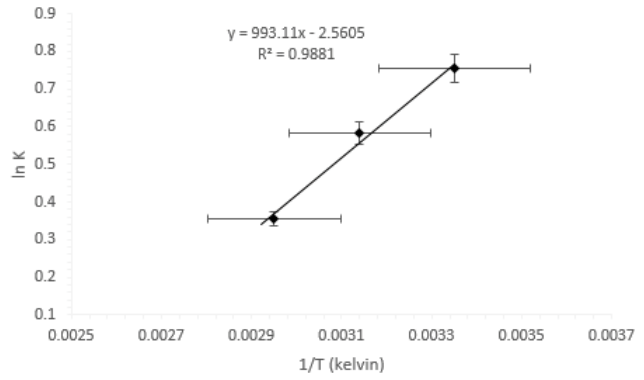

Fig. 11. Van't Hoff plot of metribuzin.

is chemical in nature. In our result the value of $\Delta G°$ lie in the range of 75–400 kJ·mol^{-1} suggest that the removal of MEB molecules on the surface of TPZnOnc is chemical adsorption.

Negative value of $\Delta H°$ (–82.56 kJ·mol^{-1}) confirms that the removal process of MEB molecules is exothermic. While negative value of $\Delta S°$ confirm that the process of randomness decreases at the solid–liquid interface for the removal of MEB molecules. Various values of thermodynamic parameters are tabulated in Table 3.

Table 3
Values of different thermodynamic parameters

Temperature (K)	$\Delta G°$ (kJ·mol^{-1})	$\Delta H°$ (kJ·mol^{-1})	$\Delta S°$ (kJ·mol^{-1})
298	–76.21		
318	–75.78	–82.56	–0.02128
338	–75.36		

Table 4
Comparison of adsorption capability of TPZnOnc with other sorbents

Sorbent	Adsorption capability (mg·g^{-1})	References
Coconut shell biochar (treated)	10.33	[36]
Coconut shell biochar (untreated)	9.66	[36]
Corn cob	4.07	[37]
TPZnOnc	19.20	Current study

3.1. Comparison with other sorbents

Table 4 shows the comparison of adsorption capability of TPZnOnc with other sorbents [36,37]. From the table it is clear that TPZnOnc is an efficient sorbent to preferably used in the removal of pesticides/pollutants from aquatic media.

3.2. Mechanism of MEB sorption on the surface of TPZnOnc

Fig. 12 explain the sorption mechanism of MEB molecules on to TPZnOnc. Various processes involved in the sorption process are:

- Complex formation: As TPZnOnc nanocomposite contain Zn metal, while insecticide (MEB) contain electron donating agents like –NH_2, –S–R and –C=O groups. All these groups can form a complex with Zn-metal atom/ion.
- Hydrogen bonding: The FTIR spectra of TPZnOnc confirm the presence of –NH_2 group and –OH group. All these groups form H-bonding with anionic sites like oxygen, nitrogen and sulphur of MEB molecules.
- Electrostatic forces of attractions: The electrostatic forces of attractions are possible between –C=O, –NH_2 and –S–CH_3 groups of TPZnOnc and different types of anionic groups on MEB.
- π–π interaction: π–π interaction may occur between pi-electrons of TPZnOnc (as electron donating species) and the pi-electronic cloud of aromatic ring of MEB molecule.

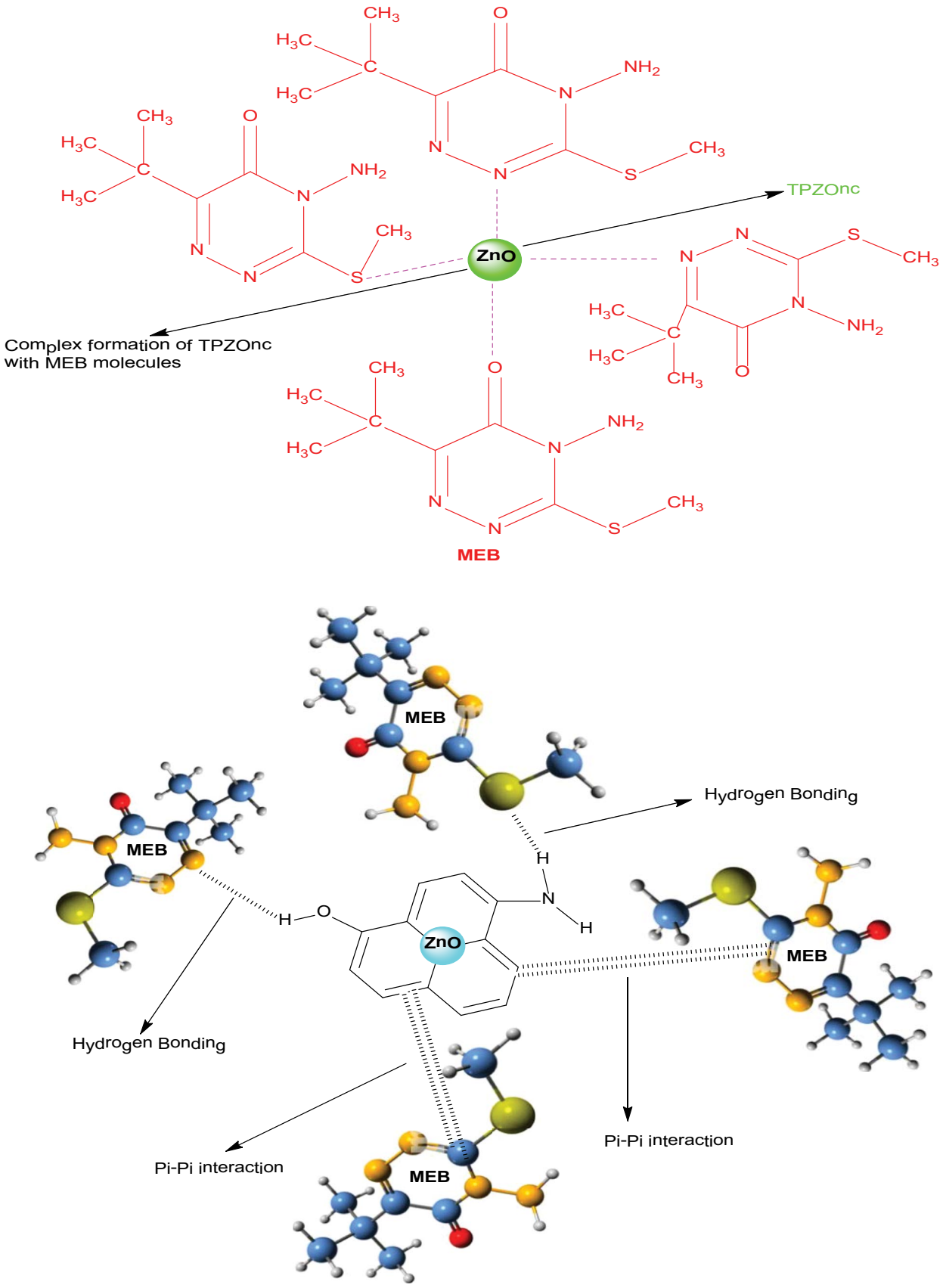

Fig. 12. Mechanism of metribuzin adsorption on the surface of TPZnOnc.

4. Conclusion

herein an efficient sorbent abbreviated as TPZnOnc was prepared from biomass precursors of turnip peels. The prepared nanocomposite was characterized using SEM, XRD and FTIR techniques. Mass titration method was used for the determination of pH_{pzc}. The pH_{pzc} of TPZnOnc was found to be 7.8. The prepared nanocomposite was then utilized for the decontamination of MEB present in solution. Maximum MEB percent removal occurred at pH 3. The optimum doze of TPZnOnc was found to be 600 mg. Different kinetic and isotherm models were employed to the adsorption kinetics and isotherm data. It was established that pseudo-second-order kinetics and Langmuir adsorption isotherm model were the best one to fitted well the adsorption kinetics and isotherm data, respectively. Negative values of $\Delta G°$ at different temperatures showed that the removal of MEB molecules on TPZnOnc to be a spontaneous and chemical process. Negative value of $\Delta H°$ suggested that the process of sorption was an exothermic process. The negative value of $\Delta S°$ confirmed the decrease in randomness at the solid–liquid interface during the process. It was concluded from the results that TPZnOnc can be effectively used as sorbent for the decontamination of a large number of contaminants from aquatic media.

Acknowledgement

The authors extend their appreciation to the researchers supporting Project number (RSP2023R110) King Saud University, Riyadh, Saudi Arabia, for financial support.

References

[1] A. Alengebawy, S.T. Abdelkhalek, S.R. Qureshi, M.-Q. Wang, Heavy metals and pesticides toxicity in agricultural soil and plants: ecological risks and human health implications, Toxics, 9 (2021) 42, doi: 10.3390/toxics9030042.
[2] K. Narita, Y. Matsui, T. Matsushita, N. Shirasaki, Selection of priority pesticides in Japanese drinking water quality regulation: validity, limitations, and evolution of a risk prediction method, Sci. Total Environ., 751 (2021) 141636, doi: 10.1016/j.scitotenv.2020.141636.
[3] V.P. Konstantinos, J.K. Anastasios, Removal of pesticides from water by NF and RO membranes — a review, Desalination, 287 (2012) 255–265.
[4] A.Q. Wahla, S. Iqbal, S. Anwar, S. Firdous, J.A. Mueller, Optimizing the metribuzin degrading potential of a novel bacterial consortium based on Taguchi design of experiment, J. Hazard. Mater., 366 (2019) 1–9.
[5] E.F.G.C. Dores, S. Navickiene, M.L.F. Cunha, L. Carbo, M.L. Ribeiro, E.M. De-Lamonica-Freire, Multiresidue determination of herbicides in environmental waters from Primavera do Leste Region (Middle West of Brazil) by SPE-GC-NPD, J. Braz. Chem. Soc., 17 (2006) 866–873.
[6] M. Essandoh, D. Wolgemuth, C.U. Pittman, D. Mohan, T. Mlsna, Adsorption of metribuzin from aqueous solution using magnetic and nonmagnetic sustainable low-cost biochar adsorbents, Environ. Sci. Pollut. Res., 24 (2017) 4577–4590.
[7] A. ul Haq, M. Saeed, M. Muneer, M.A. Jamal, T. Maqbool, T. Tahir, Biosorption of metribuzin pesticide by Cucumber (*Cucumis sativus*) peels-zinc oxide nanoparticles composite, Sci. Rep., 12 (2022) 5840, doi: 10.1038/s41598-022-09860-z.
[8] S.F.B. Suboh, S.H. Mohd-Setapar, M.B. Alshammari, A. Ahmad, Utilization of *Trametes versicolor* for the production of laccase and its application in oxytetracycline degradation from wastewater, Desal. Water Treat., 266 (2022) 284–290.
[9] S. Kostopoulou, G. Ntatsi, G. Arapis, K.A. Aliferis, Assessment of the effects of metribuzin, glyphosate, and their mixtures on the metabolism of the model plant *Lemna minor* L. applying metabolomics, Chemosphere, 239 (2020) 124582, doi: 10.1016/j.chemosphere.2019.124582.
[10] M.S. Sharifzadeh, G. Abdollahzadeh, The impact of different education strategies on rice farmers' knowledge, attitude and practice (KAP) about pesticide use, J. Saudi Soc. Agric. Sci., 20 (2021) 312–323.
[11] X. Huang, H. Zhang, F. Chen, M. Song, Colonization of *Paracoccus* sp. QCT6 and enhancement of metribuzin degradation in maize rhizosphere soil, Curr. Microbiol., 75 (2018) 156–162.
[12] A. ul Haq, J. Shah, M.R. Jan, S. ud Din, Kinetic, equilibrium and thermodynamic studies for the sorption of metribuzin from aqueous solution using banana peels, an agro-based biomass, Toxicol. Environ. Chem., 97 (2015) 124–134.
[13] H. Katsumata, T. Kobayashi, S. Kaneco, T. Suzuki, K. Ohta, Degradation of linuron by ultrasound combined with photo-Fenton treatment, Chem. Eng. J., 166 (2011) 468–473.
[14] L.J. Banasiak, B. Van der Bruggen, A.I. Schäfer, Sorption of pesticide endosulfan by electrodialysis membranes, Chem. Eng. J., 166 (2011) 233–239.
[15] M. Uğurlu, M.H. Karaoğlu, TiO_2 supported on sepiolite: preparation, structural and thermal characterization and catalytic behaviour in photocatalytic treatment of phenol and lignin from olive mill wastewater, Chem. Eng. J., 166 (2011) 859–867.
[16] T. Zhou, T.T. Lim, S.S. Chin, A.G. Fane, Treatment of organics in reverse osmosis concentrate from a municipal wastewater reclamation plant: feasibility test of advanced oxidation processes with/without pretreatment, Chem. Eng. J., 166 (2011) 932–939.
[17] M.I. Maldonado, S. Malato, L.A. Pérez-Estrada, W. Gernjak, I. Oller, X. Doménech, J. Peral, Partial degradation of five pesticides and an industrial pollutant by ozonation in a pilot-plant scale reactor, J. Hazard. Mater., 138 (2006) 363–369.
[18] H.R. Murthy, H.K. Manonmani, Aerobic degradation of technical hexachlorocyclohexane by a defined microbial consortium, J. Hazard. Mater., 149 (2007) 18–25.
[19] A.U. Haq, M. Saeed, M. Usman, M. Muneer, S. Adeel, S. Abbas, A. Iqbal, Removal of butachlor from aqueous solution using cantaloupe seed shell powder: kinetic, equilibrium and thermodynamic studies, Int. J. Environ. Sci. Technol., 16 (2019) 6029–6042.
[20] A. ul Haq, M. Saeed, M. Usman, A.F. Zahoor, M.N. Anjum, T. Maqbool, S. Naheed, M. Kashif, Mechanisms of halosulfuron methyl pesticide biosorption onto neem seeds powder, Sci. Rep., 11 (2021) 9960, doi: 10.1038/s41598-021-88929-7.
[21] S. Muhammad, U. Muhammad, M. Majid, M. Tahir, M.K.K. Khosa, A. Nasir, Performance and mechanism of removal of atrazine pesticide from aqueous media utilizing pumpkin seeds shell powder, Desal. Water Treat., 160 (2019) 229–239.
[22] A. ul Haq, M. Saeed, M. Usman, S.A.R. Naqvi, T.H. Bokhari, T. Maqbool, H. Ghaus, T. Tahir, H. Khalid, Sorption of chlorpyrifos onto zinc oxide nanoparticles impregnated Pea peels (*Pisum sativum* L): equilibrium, kinetic and thermodynamic studies, Environ. Technol. Innovation, 17 (2020) 100516, doi: 10.1016/j.eti.2019.100516.
[23] T.R. de Aguiar Jr., J.O.A. Guimarães Neto, U. Şen, H. Pereira, Study of two cork species as natural biosorbents for five selected pesticides in water, Heliyon, 5 (2019) e01189, doi: 10.1016/j.heliyon.2019.e01189.
[24] N. Singh, Adsorption of herbicides on coal fly ash from aqueous solutions, J. Hazard. Mater., 168 (2009) 233–237.
[25] S. Boudesocque, E. Guillon, M. Aplincourt, F. Martel, S. Noël, Use of a low-cost biosorbent to remove pesticides from wastewater, J. Environ. Qual., 37 (2008) 631–638.
[26] M. Akhtar, S.M. Hasany, M.I. Bhanger, S. Iqbal, Low-cost sorbents for the removal of methyl parathion pesticide from aqueous solutions, Chemosphere, 66 (2007) 1829–1838.
[27] C.S. Castro, M.C. Guerreiro, M. Gonçalves, L.C. Oliveira, A.S. Anastácio, Activated carbon/iron oxide composites for the

removal of atrazine from aqueous medium, J. Hazard. Mater., 164 (2009) 609–614.
[28] V.M. Boddu, K. Abburi, J.L. Talbott, E.D. Smith, Removal of hexavalent chromium from wastewater using a new composite chitosan biosorbent, Environ. Sci. Technol., 37 (2003) 4449–4456.
[29] I. Michalak, K. Chojnacka, A. Witek-Krowiak, State of the art for the biosorption process a review, Appl. Biochem. Biotechnol., 170 (2013) 1389–1416.
[30] V.K. Mourya, N.N. Inamdar, Chitosan-modifications and applications: opportunities galore, React. Funct. Polym., 68 (2008) 1013–1051.
[31] K.B. Angelin, S. Siva, R.S. Kannan, Zinc oxide nanoparticles impregnated polymer hybrids for efficient extraction of heavy metals from polluted aqueous solution, Asian J. Sci. Technol., 6 (2015) 2139–2150.
[32] B. Rahmanifar, S. Moradi Dehaghi, Removal of organochlorine pesticides by chitosan loaded with silver oxide nanoparticles from water, Cleaner Technol. Environ. Policy, 16 (2014) 1781–1786.
[33] N. Ayawei, A.N. Ebelegi, D. Wankasi, Modelling and interpretation of adsorption isotherms, J. Chem., 2017 (2017) 3039817, doi: 10.1155/2017/3039817.
[34] A.V. Kiselev, Adsorption of vapours when complexes of adsorbate molecules are formed on the surface, Colloids J., 20 (1958) 338–348.
[35] M.R. Mafra, L. Igarashi-Mafra, D.R. Zuim, É.C. Vasques, M.A. Ferreira, Adsorption of Remazol brilliant blue on an orange peel adsorbent, Braz. J. Chem. Eng., 30 (2013) 657–665.
[36] N.A. Baharum, H.M. Nasir, M.Y. Ishak, N.M. Isa, M.A. Hassan, A.Z. Aris, Highly efficient removal of diazinon pesticide from aqueous solutions by using coconut shell-modified biochar, Arabian J. Chem., 13 (2020) 6106–6121.
[37] B. Ara, J. Shah, M. Rasul Jan, S. Aslam, Removal of metribuzin herbicide from aqueous solution using corn cob, Int. J. Sci. Environ., 2 (2013) 146–161.